High-Pressure Single-Crystal X-ray Diffraction Study of Two Spin-Crossover Iron(II) Complexes: $Fe(Phen)_2(NCS)_2$ and $Fe(Btz)_2(NCS)_2$

Thierry Granier,*[1a] Bernard Gallois,[1a] Jacques Gaultier,[1a] José-Antonio Real,*[1b] and Jacqueline Zarembowitch*[1c]

Laboratoire de Cristallographie et de Physique Cristalline, CNRS URA 144, Université Bordeaux I, 33405-Talence Cedex, France, Departament de Quimica Inorganica, Universitat de València, 46100 Burjassot, Spain, and Laboratoire de Chimie Inorganique, CNRS URA 420, Université Paris-Sud, 91405 Orsay, France

*Received February 17, 1993**

Crystal structures of $Fe(Phen)_2(NCS)_2$, form II (phen = 1,10-phenanthroline) and $Fe(Btz)_2(NCS)_2$ (Btz = 2,2'-bi-4,5-dihydrothiazine) were determined at room temperature by X-ray diffraction, under a pressure of $P \simeq 1.0$ GPa. For both compounds, the space group is orthorhombic, *Pbcn* ($Z = 4$). Lattice constants of $Fe(Phen)_2(NCS)_2$ are $a = 12.656(3)$, $b = 9.848(2)$, and $c = 16.597(4)$ Å. Data were refined (159 parameters) to $R_w = 0.043$ for 631 observed reflections ($F_o > 4\sigma(F_o)$); for $Fe(Btz)_2(NCS)_2$, $a = 12.839(4)$, $b = 10.454(3)$, and $c = 16.362(4)$ Å, with $R_w = 0.056$ (154 parameters for 662 observed reflections). Both structures reveal that the iron(II) complexes are in the low-spin state. The molecular configurations are very similar to those obtained at ambient pressure and low temperature: similar shortenings of Fe–N(ligand) bond lengths as well as a more regular shape of the [$Fe–N_6$] octahedra are observed, compared to those at ambient pressure and room temperature. Lattice parameters have been obtained over the pressure range [1000 HPa to 1.3 GPa]: a pronounced change of derivative in the curve a vs P relative to $Fe(Phen)_2(NCS)_2$ is clearly evidenced at $P_c \simeq 0.6$ GPa, the pressure at which the singlet-quintet spin transition is expected to occur, according to recent high-pressure magnetic susceptibility, infrared, and X-ray absorption studies. $Fe(Btz)_2(NCS)_2$ does not reveal such a lattice parameter anomaly. Only a slight change of slope in the curve representing the evolution of the unit cell volume as a function of pressure is observed at 0.4–0.5 GPa. The spin conversion is found to occur more gradually in the latter compound than in the former. Compressibility data are used to estimate the volume variation associated with the spin transition in the case of $Fe(Phen)_2(NCS)_2$: it is very close to the one obtained as a function of temperature. Bulk moduli are comparable for both complexes, but $Fe(Phen)_2(NCS)_2$ exhibits a strong lattice anisotropy compared to $Fe(Btz)_2(NCS)_2$. These parameters are discussed in relation with the cooperativity of the spin transition.

Introduction

The most abrupt thermally induced low-spin (LS) ↔ high-spin (HS) transitions reported up to now are those exhibited by a number of iron(II) complexes.[2,3] These compounds are all the more attractive as, when a thermal hysteresis is associated with the transition, they are bistable in the temperature range delimited by the hysteresis loop and may therefore present a memory effect.[4] However, the molecular and crystalline parameters which govern the cooperativity of the phenomenon are not yet completely specified. The results relative to $Fe(Phen)_2(NCS)_2$ and $Fe(Btz)_2(NCS)_2$ we report in this paper are part of work we have undertaken in order to better know the nature and the "weight" of these parameters.

$Fe(Phen)_2(NCS)_2$ and $Fe(Btz)_2(NCS)_2$ have been known for a long time to exhibit a $^5T_2 \leftrightarrow {}^1A_1$ spin conversion in the solid state, at low temperature.[5,6]

$Fe(Phen)_2(NCS)_2$ has certainly been one of the most investigated iron(II) spin-transition complexes and therefore can be considered as a reference compound in this family. Under atmospheric pressure, it undergoes an abrupt HS ↔ LS transition at a temperature $T_c \simeq 176$ K.[7,8] Various techniques were used to study this transition such as magnetic susceptibility measurements, Mössbauer, IR, and UV–visible spectrometries, X-ray powder diffraction and absorption, and calorimetric measurements (see ref 9 and references therein). On the other hand, more limited have been the investigations under pressure effect: these concern IR[10,11], UV–visible,[12] Mössbauer,[12,13] and X-ray absorption[14] spectrometry experiments, whereas the only experiments conducted under conjugated temperature and pressure effects have been magnetic susceptibility measurements.[15] Though all the results which were obtained agree with the occurrence of a HS ↔ LS spin conversion under pressure, the critical pressure P_c of the spin transition is not properly defined and authors still disagree on its value at room temperature: $P_c \simeq 0.6$,[15] 0.8,[11] 1.35,[13] or 1.2 GPa.[12] It was shown recently that $Fe(Phen)_2(NCS)_2$ can exist in two crystalline forms (named I and II),[9] depending on the method used for preparing the compound. On this basis, it can be stated that the samples studied in refs 10 and 15 were in form I. In refs 11 and 12, the method of synthesis is not specified. The present work is related to crystals in form II.

Less attention, on the other hand, has been devoted to $Fe(Btz)_2(NCS)_2$. To our knowledge, this compound has been studied so far only as a function of temperature: it undergoes a HS ↔

* Abstract published in *Advance ACS Abstracts*, October 1, 1993.

(1) (a) Université de Bordeaux I, (b) Universitat de València. (c) Université de Paris-Sud.
(2) Gütlich, P. *Struct. Bonding* **1981**, *44*, 83.
(3) König, E.; Ritter, G.; Kulshreshtha, S. K. *Chem. Rev.* **1985**, *85*, 219.
(4) Zarembovitch, J.; Kahn, O. *New J. Chem.* **1991**, *15*, 181.
(5) Baker, W. A.; Bobonich, H. M. *Inorg. Chem.* **1964**, *3*, 1184.
(6) Bradley, G.; McKee, V.; Nelson, S. M.; Nelson, J. *J. Chem. Soc.* **1978**, 522.
(7) König, E.; Madeja, K. *Chem. Commun.* **1966**, *3*, 61.
(8) Sorai, M.; Seki, S. *J. Phys. Chem. Solids* **1974**, *35*, 555.
(9) Gallois, B.; Real, J. A.; Hauw, C.; Zarembowitch, J. *Inorg. Chem.* **1990**, *29*, 1152.
(10) Ferraro, J. R.; Takemoto, J. *J. Appl. Spectrosc.* **1974**, *28*, 66.
(11) Adams, D. M.; Long, G. J.; Williams, A. D. *Inorg. Chem.* **1982**, *21*, 149.
(12) Fisher, D. C.; Drickamer, H. G. *J. Chem. Phys.* **1971**, *54*, 4825.
(13) Pebler, J. *Inorg. Chem.* **1983**, *22*, 4125.
(14) Roux, C.; Zarembowitch, J.; Itié, J. P.; Polian, A.; Verdaguer, M.; Claude, R.; Dartyge, E.; Fontaine, A.; Tolentino, E. To be submitted for publication.
(15) Usha, S.; Srinivasan, R.; Rao, C. N. R. *Chem. Phys.* **1985**, *100*, 447.

0020-1669/93/1332-5305$04.00/0

LS conversion over a wide temperature range centered around $T_c \simeq 215$ K,[6] a temperature at which HS and LS isomers are in a nearly equivalent ratio.

Although much information could be obtained concerning the physical behavior of these two compounds, it is only recently that new methods of preparation, yielding single crystals of suitable size, allowed us to achieve a full X-ray diffraction investigation.[9,16,17] From preliminary room temperature data, it was found that $Fe(Phen)_2(NCS)_2$ and $Fe(Btz)_2(NCS)_2$ are isostructural: they crystallize in the same space group and exhibit the same molecular packing. On the basis of this similitude, it appeared that a comparative structural investigation of both compounds as a function of temperature or pressure could reveal new insights concerning the relationship between their magnetic and structural properties. The structural investigation we performed on both complexes as a function of temperature, including structure determinations at room temperature and low temperature, and a thermal expansion study[9,16,17] allowed one to bring out important information concerning the structural properties of these two compounds, with respect to the difference in their magnetic behaviors.

In this paper, we report a similar X-ray structural investigation on both compounds, conducted at room temperature, as a function of pressure. To our knowledge, this is the first high-pressure single-crystal X-ray diffraction investigation performed on spin-transition iron(II) complexes.

In the following, we first describe the crystal structures obtained at $P \simeq 1.0$ GPa and $P \simeq 0.95$ GPa for $Fe(Phen)_2(NCS)_2$ and $Fe(Btz)_2(NCS)_2$, respectively, then we compare the intramolecular and intermolecular modifications with those observed, under atmospheric pressure, when passing from room to low temperature. Thermal dilatation data have clearly shown[17] that the variation of lattice parameters is strongly correlated with the evolution of the magnetic susceptibility, and hence of the HS fraction, as a function of temperature. In the same way, we report the compressibility data obtained for both complexes over the pressure range 1000 HPa to 1.3 GPa, in order to correlate the lattice behavior with the physical properties, and we discuss some structural parameters which have been suggested to play a relevant role in the magnetic behavior of these compounds, such as the volume variation upon the spin transition, the bulk modulus, and the compressibility tensor.[3,18-21]

Experimental Section

Materials. Single crystals were obtained according to the procedures described previously.[9,17] Dimensions of the crystals used for these experiments were $0.13 \times 0.20 \times 0.10$ mm^3 for $Fe(Phen)_2(NCS)_2$ and $0.12 \times 0.15 \times 0.10$ mm^3 for $Fe(Btz)_2(NCS)_2$.

High-Pressure X-ray Diffraction. Experiments were performed with a gasketed diamond-anvil cell designed by Ahsbahs[22] and mounted on a single-crystal X-ray diffractometer. The pressure-transmitting medium was Fluorinert FC75 (C_8F_{18}) (Fluorinert is a trademark of the 3M Co.). Pressure in the cell was measured from the shift ($d\lambda/dP = 42.6 \times 10^{-2}$ Å MPa^{-1}) of the optical absorption maximum ($\lambda_0 = 5270$ Å at P = 1000 HPa) of Ni(dimethylglyoximine)$_2$, with an estimated accuracy of 0.05 GPa.[23]

Table I. Crystallographic Data

$Fe(Phen)_2(NCS)_2$	
chem formula: $C_{26}H_{16}N_6S_2Fe$	fw = 532.4
$a = 12.656(3)$ Å	space group = *Pbcn* (No. 60)
$b = 9.848(2)$ Å	$T = 293$ K; $P = 1.0$ GPa
$c = 16.597(4)$ Å	λ(Mo Kα) = 0.710 69 Å
$V = 2068.5$ Å^3	$\rho_{obs} = 1.710$ g cm^{-3}
$Z = 4$	$\mu = 16.39$ cm^{-1}
$R^a = 0.055$	$R_w{}^a = 0.043$
$Fe(Btz)_2(NCS)_2$	
chem formula: $C_{18}H_{24}N_6S_6Fe$	fw = 572.6
$a = 12.839(4)$ Å	space group = *Pbcn* (No. 60)
$b = 10.454(3)$ Å	$T = 293$ K; $P = 0.95$ GPa
$c = 16.362(4)$ Å	λ(Mo Kα) = 0.710 69 Å
$V = 2196.7$ Å^3	$\rho_{obs} = 1.732$ g cm^{-1}
$Z = 4$	$\mu = 18.95$ cm^{-1}
$R^a = 0.058$	$R_w{}^a = 0.056$

$^a R = \sum[|F_o| - |F_c|]/\sum|F_o|$. $R_w = \sum w^{1/2}[|F_o| - |F_c|]/\sum w^{1/2}|F_o|$.

Unit cell parameters were obtained, for $Fe(Phen)_2(NCS)_2$ and $Fe(Btz)_2(NCS)_2$, respectively, at 23 (21) different pressures from the observed angular positions of 15 (16) centered Bragg reflections ($20° < \theta < 30°$). At $P = 1.0$ GPa (0.95 GPa), 1629 (1723) independent Bragg reflection intensities were collected on a STOE diffractometer (lifting counter technique; equi-inclination Weissenberg geometry; c axis parallel to the instrument axis; ω scan; Mo Kα radiation) according to an already-described method (see refs 24 and 25). Details on crystal data and data collections for both compounds are summarized in Table I. Data reduction was carried out taking into account beryllium and diamond parasitic scattering (inhomogeneous background). Lorentz and polarization corrections have been applied. According to the small crystal sizes used, no absorption correction was taken into account. The particular data reduction procedure[24] led to select 631 (662) observed reflections of reliable quality ($F_o > 4\sigma(F_o)$) for least square refinement. This refinement was carried out using the program SHELX76[26] with, as starting values, the HS phase atomic coordinates[9,17] at room temperature and atmospheric pressure. The number of observed reflections used for refinement is less important than the one taken into account at atmospheric pressure, i.e. 1050 (1115). This is a common feature in such experiments: various factors (such as the framework of the pressure cell, which reduces the reciprocal space investigated, the beryllium gasket, and the diamond anvils, which increase the diffuse background) lead to a lower but still acceptable value for the ratio of the number of observed reflections to the number of refined parameters ($\simeq 3$ for $Fe(Phen)_2(NCS)_2$, $\simeq 4$ for $Fe(Btz)_2(NCS)_2$). Atomic scattering factors were taken from ref 27. Final reliability factors were $R_w = 0.043$ and $R_w = 0.058$ for $Fe(Phen)_2(NCS)_2$ and $Fe(Btz)_2(NCS)_2$, respectively. Fractional atomic coordinates and equivalent isotropic temperature factors are given in Tables II and III.

High-Pressure Structures

For both compounds, no change of symmetry was observed in the range 1000 HPa to 1.3 GPa: the space group remains orthorhombic, *Pbcn*, and the molecular packings remain very similar to the corresponding ones observed at ambient pressure, either at room or at low ($T \simeq 130$ K) temperature. Figure 1a,b gives a projection along the a axis of the crystal structures: the molecular packing is made of sheets of complex molecules parallel to the (a,b) plane, which stack along the c axis. In the following paragraph, we present the molecular configuration of each compound, and then we discuss the intermolecular interactions observed at high pressure.

1. Molecular Configuration. Figure 2a,b shows the molecular units and the labeling of atoms for each complex. Let us recall that, in both cases, the iron atom is located on a 2-fold axis, and that, as a consequence, two similar ligands belonging to the same

(16) Gallois, B.; Granier, T.; Suez-Panama, F.; Real, J. A.; Zarembowitch, J. *Phase Transitions* **1991**, *32*, 193.
(17) Real, J. A.; Gallois, B.; Granier, T.; Suez-Panama, F.; Zarembowitch, J. *Inorg. Chem.* **1992**, *31*, 4972.
(18) König, E.; Ritter, G.; Irler, W.; Goodwin, H. A. *J. Am. Chem. Soc.* **1980**, *102*, 4681.
(19) Spiering, H.; Meissner, E.; Köppen, H.; Müller, E. W.; Gütlich, P. *Chem. Phys.* **1982**, *68*, 65.
(20) Wiehl, L.; Kiel, G.; Köhler, C. P.; Spiering, H.; Gütlich, P. *Inorg. Chem.* **1986**, *25*, 1565.
(21) Adler, P.; Wiehl, L.; Meissner, E.; Köhler, C. P.; Spiering, H.; Gütlich, P. *J. Phys. Chem. Solids*, **1987**, *48*, 517.
(22) Ahsbahs, H. *Rev. Phys. Appl.* **1984**, *19*, 819.
(23) Davies, H. W. *J. Res. Natl. Bur. Stand., Sect. A* **1968**, *72*, 149.
(24) Loumrhari, H. Thesis No. 1864, University of Bordeaux I, France, 1983.
(25) Gallois, B.; Gaultier, J.; Hauw, C.; Lamcharfi, T.; Filhol, A. *Acta Crystallogr.* **1986**, *B42*, 564.
(26) Sheldrick, G. M., SHELX76. Program for Crystal Structure Determination. University of Cambridge, England, 1976.
(27) *International Tables for X-ray Crystallography*; Kynoch Press: Birmingham, England, 1974; Vol. 4, p 99.

Table II. $Fe(Phen)_2(NCS)_2$ (P = 1.0 GPa; T = 293 K): Fractional Atomic Coordinates (×10⁴)[a] and Isotropic Thermal Parameters (Å² × 10³) for Non-Hydrogen Atoms

	x/a	y/b	z/c	U_{eq}[b]
Fe	0(0)	6550(2)	2500(0)	28(1)
N(1)	-1543(6)	6383(8)	2749(4)	23(1)
N(2)	120(6)	5148(9)	3347(5)	26(1)
N(20)	302(5)	7943(7)	3306(5)	15(1)
C(1)	-1722(7)	5369(10)	3281(7)	28(3)
C(2)	-809(8)	4741(10)	3632(6)	25(3)
C(3)	-2359(7)	7004(9)	2410(7)	15(3)
C(4)	-3406(7)	6691(10)	2622(7)	24(3)
C(5)	-3614(8)	5680(11)	3168(7)	27(3)
C(6)	-2754(7)	4989(11)	3508(6)	28(3)
C(7)	-2856(8)	3893(10)	4090(7)	37(4)
C(8)	-1991(7)	3292(12)	4427(7)	29(4)
C(9)	-929(8)	3693(9)	4206(6)	37(4)
C(10)	-21(10)	3160(9)	4526(6)	30(4)
C(11)	937(7)	3637(11)	4293(7)	37(10)
C(12)	988(7)	4646(9)	3692(6)	24(12)
C(21)	728(8)	8731(10)	3707(7)	29(1)
S(22)	1300(2)	9840(3)	4286(2)	35(6)

[a] Numbers in parentheses are estimated standard deviations in the least significant digit. [b] Values for anisotropically refined atoms are given in the form of the equivalent isotropic thermal parameters U_{eq} = $(1/3)(U_{11} + U_{22} + U_{33})$.

Table III. $Fe(Btz)_2(NCS)_2$ (P = 0.95 GPa; T = 293 K): Fractional Atomic Coordinates (×10⁴)[a] and Isotropic Thermal Parameters (Å² × 10³) for Non-Hydrogen Atoms

	x/a	y/b	z/c	U_{eq}[b]
Fe	0(0)	5815(2)	2500(1)	30(2)
N(1)	-1403(6)	5693(8)	2985(6)	33(5)
N(2)	276(6)	4549(7)	3363(6)	31(5)
N(20)	399(8)	7176(8)	3249(6)	41(5)
C(1)	-1497(8)	4930(10)	3584(7)	32(6)
C(2)	-490(9)	4292(9)	3829(8)	46(6)
C(3)	-2291(8)	6442(11)	2673(7)	45(6)
C(4)	-3303(11)	6175(17)	3119(13)	113(6)
C(5)	-3522(11)	5488(15)	3708(11)	125(6)
C(8)	750(9)	2791(10)	4785(7)	46(6)
C(9)	1279(9)	2729(9)	4003(6)	36(6)
C(10)	1291(8)	4015(10)	3531(8)	41(6)
C(21)	682(8)	8078(10)	3581(7)	34(6)
S(6)	-2589(3)	4502(4)	4154(3)	68(3)
S(7)	-544(3)	3454(3)	4744(2)	48(3)
S(22)	1099(3)	9375(3)	4048(3)	55(3)

[a] Numbers in parentheses are estimated standard deviations in the least significant digit. [b] Values for anisotropically refined atoms are given in the form of the equivalent isotropic thermal parameters U_{eq} = $(1/3)(U_{11} + U_{22} + U_{33})$.

molecular unit deduce from each other by this axis. Bond lengths and bond angles are listed in Tables IV and V for $Fe(Phen)_2(NCS)_2$ and $Fe(Btz)_2(NCS)_2$, respectively.

a. [Fe–N_6] Core Geometry. Compared to ambient pressure and room temperature values, the most noticeable intramolecular modifications concern the iron octahedral environment: Fe–N(ligand) bond lengths and N–Fe–N bond angles observed for both compounds at room temperature and low temperature under atmospheric pressure and at room temperature under high-pressure are reported in Table VI. One clearly notices that high-pressure values are very close to the values obtained for the LS phase at 130 K: for each compound, Fe–N(ligand) bond lengths of the high-pressure and low-temperature structures do not differ by more than 0.03 Å. Similarly, the differences observed in bond angles are not larger than 1.5°.

According to the data mentioned in Table VI, the geometry of the [Fe–N_6] octahedron under pressure is found to be nearly the same as the one obtained at low temperature (130 K): an average shortening of 0.22 and 0.20 Å for Fe–N(Phen) and Fe–N(Btz) bond lengths, a reduced shortening of 0.10 and 0.12 Å for Fe–N(CS) distances, and variations of 1.0–7.1° for N–Fe–N angles lead to a more regular shape for [Fe–N_6] octahedra. The

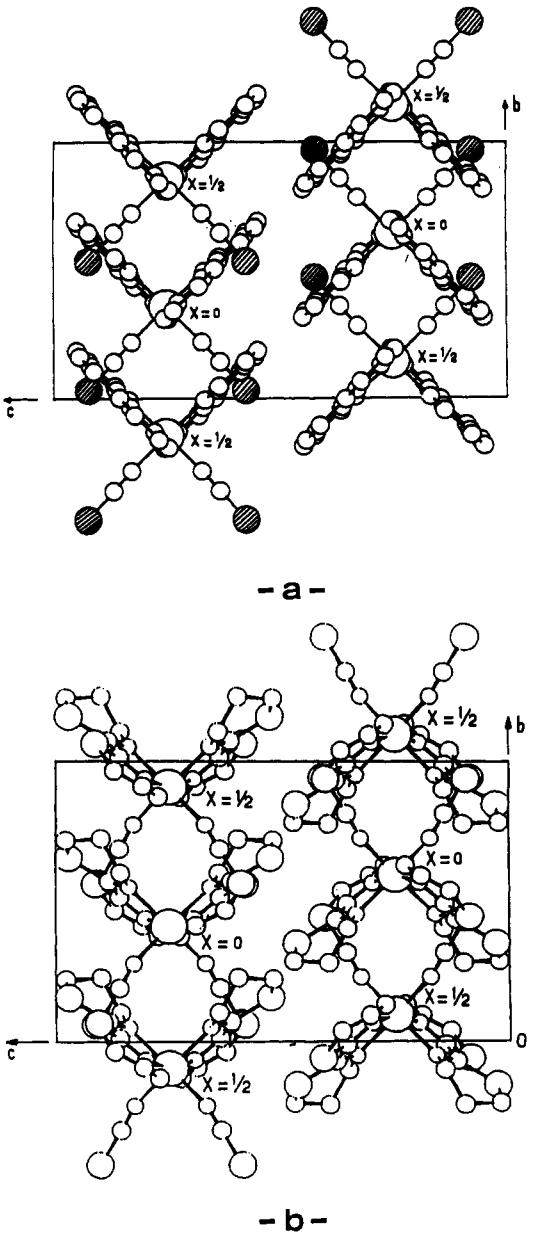

Figure 1. Projection along the a axis of the crystal structures of (a) $Fe(Phen)_2(NCS)_2$ and (b) $Fe(Btz)_2(NCS)_2$.

similarity of coordination core geometries at high pressure and low temperature suggests that, under a pressure of 1.0 GPa, both $Fe(Phen)_2(NCS)_2$ and $Fe(Btz)_2(NCS)_2$ compounds have reached the LS state, even if no physical data support this statement in the case of $Fe(Btz)_2(NCS)_2$,. However, concerning $Fe(Phen)_2(NCS)_2$, this result can be compared with those obtained when studying other physical properties under the same conditions. More precisely, this poses the problem of the discrepancies in the values of the transition critical pressure (P_c) obtained so far for this compound, values which lie between 0.6 and 1.4 GPa as seen above: our full structural determination seems to show that P_c is lower than 1.0 GPa.

In the last section, we present the compressibility data obtained on both compounds in the range 1000 HPa to 1.3 GPa. We show that a thorough analysis of the evolution of lattice parameters as a function of pressure, as well as a comparison with temperature effects, allows us to define P_c in the case of $Fe(Phen)_2(NCS)_2$, and to discuss the development of the spin conversion upon the application of pressure for $Fe(Btz)_2(NCS)_2$.

b. Ligand Configuration. Only very slight modifications of ligand geometries are observed when pressure is applied.

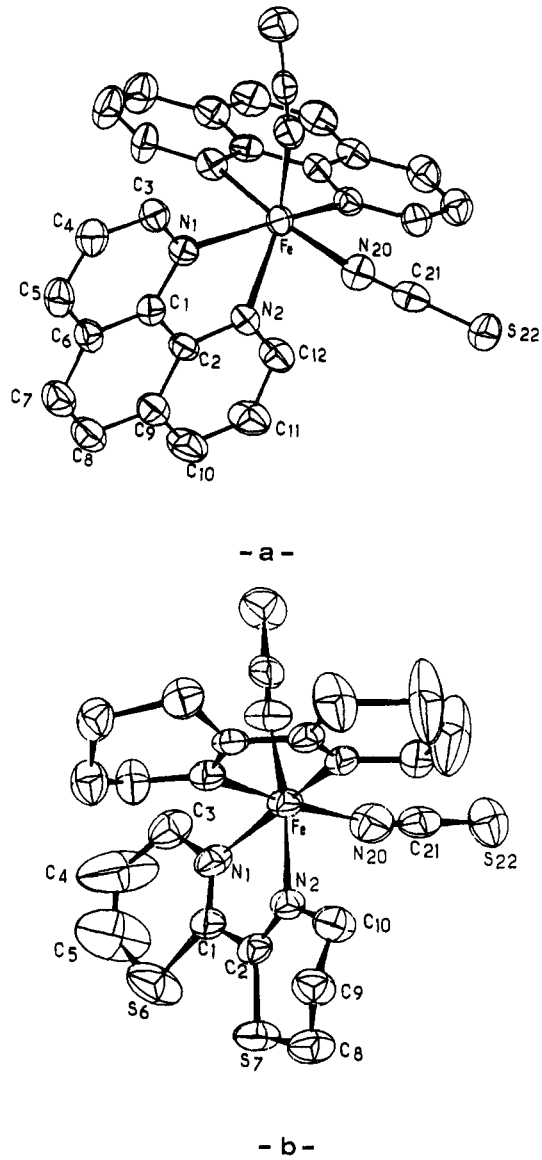

Figure 2. Drawings of the (a) $Fe(Phen)_2(NCS)_2$ and (b) $Fe(Btz)_2(NCS)_2$ units showing the 50% probability ellipsoids. Hydrogen atoms have been omitted for clarity.

In the case of $Fe(Phen)_2(NCS)_2$, a comparison of the bond lengths and bond angles obtained under pressure (Table IV) with those observed previously at 293 K and ambient pressure[9] indicates no significant difference. The most noticeable changes only affect the Fe–N(1)–C(1) bond angle (114.3° at ambient pressure; 110.7° at P = 1.0 GPa) and the N(2)–C(2)–C(1) angle (118.9° at ambient pressure; 116.0° at P = 1.0 GPa). Taking into account the esd's on these values, the N(1)–C(1)–C(2)–N(2) segment appears almost unchanged.

Moreover, the phenanthroline ligand preserves its planar configuration: the greatest deviation of Phen atoms relative to the mean molecular plane defined by C(1), C(2), C(6), C(7), C(8), and C(9) (equation of the plane: $0.0388x + 0.6979y + 0.7151z = 7.7298$) is 0.074 Å and concerns the atom C(11). Meanwhile, the angle between two phenanthroline planes belonging to the same unit is 94.5° (92.9° at ambient pressure; 91.5° at 130 K).

The NCS^- group is not distorted by the shortening of the Fe–N(20) distance: N(20)–C(21)–S(21) remains quasilinear (N(20)–C(21)–S(22) = 178.5° at 1.0 GPa, 179.4° at ambient pressure, and 179.5° at 130 K) while the Fe–N–C(S) linkage is more bent in the LS configuration: Fe–N(20)–C(21) = 163.5° at 1.0 GPa, 167.0° at ambient pressure, and 165.6° at 130 K.

Table IV. $Fe(Phen)_2(NCS)_2$ (P = 1.0 GPa; T = 293 K): Bond Distances (Å) and Bond Angles (deg)[a]

N(1)–Fe	2.003(7)	N(2)–Fe–N(1)	82.5(3)
N(2)–Fe	1.975(8)	N(20)–Fe–N(1)	95.8(3)
N(20)–Fe	1.954(7)	N(20)–Fe–N(2)	88.6(3)
C(1)–N(1)	1.352(12)	C(1)–N(1)–Fe	110.7(7)
C(3)–N(1)	1.326(12)	C(3)–N(1)–Fe	129.7(7)
C(2)–N(2)	1.329(13)	C(3)–N(1)–C(1)	119.5(8)
C(12)–N(2)	1.335(12)	C(2)–N(2)–Fe	113.7(7)
C(21)–N(20)	1.156(13)	C(12)–N(2)–Fe	129.7(7)
C(2)–C(1)	1.433(14)	C(12)–N(2)–C(2)	116.6(8)
C(9)–C(2)	1.413(14)	C(21)–N(20)–Fe	163.5(8)
C(3)–C(4)	1.405(14)	C(2)–C(1)–N(1)	116.6(9)
C(4)–C(5)	1.372(15)	C(6)–C(1)–N(1)	123.0(10)
C(1)–C(6)	1.409(15)	C(6)–C(1)–C(2)	120.3(10)
C(5)–C(6)	1.403(15)	C(1)–C(2)–N(2)	116.0(10)
C(7)–C(6)	1.455(14)	C(9)–C(2)–N(2)	124.6(10)
C(8)–C(7)	1.363(15)	C(9)–C(2)–C(1)	119.4(10)
C(9)–C(8)	1.447(15)	C(5)–C(6)–C(1)	115.5(9)
C(10)–C(9)	1.372(15)	C(7)–C(6)–C(1)	119.0(9)
C(11)–C(10)	1.356(15)	C(7)–C(6)–C(5)	125.6(10)
C(12)–C(11)	1.409(14)	C(4)–C(5)–C(6)	119.6(10)
S(22)–C(21)	1.625(11)	C(5)–C(4)–C(3)	119.3(9)
		C(4)–C(3)–N(1)	122.2(8)
		C(8)–C(7)–C(6)	122.6(9)
		C(9)–C(8)–C(7)	121.2(9)
		C(8)–C(9)–C(2)	118.3(10)
		C(10)–C(9)–C(2)	116.8(10)
		C(11)–C(10)–C(9)	118.4(8)
		C(12)–C(11)–C(10)	120.1(9)
		C(11)–C(12)–N(2)	123.3(9)
		S(22)–C(21)–N(20)	178.5(10)

[a] Numbers in parentheses are estimated standard deviations in the least significant digit.

Table V. $Fe(Btz)_2(NCS)_2$ (P = 0.95 GPa; T = 293 K): Bond Distances (Å) and Bond Angles (deg)[a]

Fe–N(1)	1.973(8)	N(1)–Fe–N(2)	80.3(4)
Fe–N(2)	1.968(9)	N(1)–Fe–N(20)	91.9(4)
Fe–N(20)	1.947(9)	N(2)–Fe–N(20)	89.5(4)
N(1)–C(3)	1.475(13)	Fe–N(1)–C(3)	122.1(7)
N(1)–C(1)	1.268(14)	Fe–N(1)–C(1)	116.0(7)
N(2)–C(2)	1.273(15)	C(3)–N(1)–C(1)	121.9(9)
N(2)–C(10)	1.443(13)	Fe–N(2)–C(2)	115.6(8)
N(20)–C(21)	1.147(14)	Fe–N(2)–C(10)	124.0(7)
C(3)–C(4)	1.517(19)	C(2)–N(2)–C(10)	120.2(9)
C(5)–C(4)	1.234(26)	Fe–N(20)–C(21)	169.1(9)
C(1)–C(2)	1.509(15)	N(1)–C(3)–C(4)	113.4(10)
C(8)–C(9)	1.450(16)	N(1)–C(1)–C(2)	113.7(9)
C(9)–C(10)	1.550(15)	S(6)–C(1)–N(1)	130.6(8)
S(6)–C(1)	1.743(11)	S(6)–C(1)–C(2)	115.7(7)
S(6)–C(5)	1.741(13)	N(2)–C(2)–C(1)	114.2(10)
S(7)–C(2)	1.737(13)	S(7)–C(2)–N(2)	130.8(9)
S(7)–C(8)	1.801(11)	S(7)–C(2)–C(1)	114.8(8)
C(21)–S(22)	1.646(11)	C(3)–C(4)–C(5)	132.7(16)
		C(4)–C(5)–S(6)	121.0(11)
		C(9)–C(8)–S(7)	114.6(8)
		C(8)–C(9)–C(10)	113.9(9)
		N(2)–C(10)–C(9)	114.9(9)
		C(5)–S(6)–C(1)	100.2(6)
		C(8)–S(7)–C(2)	100.9(5)
		N(20)–C(21)–S(22)	179.3(10)

[a] Numbers in parentheses are estimated standard deviations in the least significant digit.

As far as $Fe(Btz)_2(NCS)_2$ is concerned, the bond lengths and bond angles given in Table V show that the values obtained under high pressure are very similar to those obtained at low temperature.[17] Here again, very slight modifications are observed in the btz configuration: the Fe–N(1) and Fe–N(2) shortening and the N(1)–Fe–N(2) angle increase induce no significant variation of the N(1)–C(1)–C(2)–N(2) segment.

The Btz moiety remains distorted relatively to the mean molecular plane defined by N(1), C(1), C(2), and N(2) atoms ($0.2328x + 0.7567y + 0.6109z = 7.056$): the greatest deviation (0.51 Å) concerns the atom C(9). Finally, C(5) and C(4) atoms

Table VI. Modifications of the [Fe–N_6] Octahedron Geometry under Constraint, for $Fe(Phen)_2(NCS)_2$ and $Fe(Btz)_2(NCS)_2$ (Numbers in Parentheses are Last Digit Standard Deviations)

	$Fe(Phen)_2(NCS)_2$			$Fe(Btz)_2(NCS)_2$		
	1000 HPa[a]			1000 HPa[b]		
	293 K	130 K	1.0 GPa; 293 K[c]	293 K	130 K	0.95 GPa; 293 K[c]
Fe–N(1), Å	2.199(3)	2.014(4)	2.003(7)	2.165(6)	1.982(7)	1.973(8)
Fe–N(2), Å	2.213(3)	2.005(4)	1.975(8)	2.176(6)	1.965(6)	1.968(9)
Fe–N(20), Å	2.057(4)	1.958(4)	1.954(7)	2.064(7)	1.948(8)	1.947(9)
N(1)–Fe–N(2), deg	76.1(1)	81.8(1)	82.6(3)	74.7(2)	80.3(3)	80.3(4)
N(1)–Fe–N(20), deg	103.2(1)	95.3(1)	96.1(3)	97.4(2)	91.1(3)	91.9(4)
N(2)–Fe–N(20), deg	89.6(1)	89.1(1)	90.6(3)	90.7(2)	89.7(3)	89.5(4)
N(20)–Fe–N′(20),[d] deg	94.9(1)	90.6(1)	90.7(3)	95.0(2)	90.1(3)	89.3(4)
spin state	HS	LS	LS	HS	LS	LS

[a] Reference 9. [b] Reference 17. [c] This work. [d] N′(20) is deduced from N(20) by the 2-fold axis.

Table VII. Angular Orientations (deg) of the Fe–N Bond Directions with Regard to the Principal Axes of the Lattice[a]

	$Fe(Phen)_2(NCS)_2$		$Fe(Btz)_2(NCS)_2$	
angles	1000 HPa[b]	1.0 GPa[d]	1000 HPa[c]	0.95 GPa[d]
N(1)–Fe–Ox	164.3	167.2	154.1	156.2
N(1)–Fe–Oy	99.9	94.6	89.2	93.9
N(1)–Fe–Oz	78.0	78.1	65.6	66.5
N(2)–Fe–Ox	88.3	85.6	82.2	79.5
N(2)–Fe–Oy	135.5	134.3	135.4	132.1
N(2)–Fe–Oz	46.6	44.7	46.4	44.0
N(20)–Fe–Ox	74.7	78.7	71.0	74.9
N(20)–Fe–Oy	47.4	45.4	45.8	42.9
N(20)–Fe–Oz	46.6	46.8	50.4	51.0

[a] Values at ambient pressure and 1.0 GPa (T = 293 K) for $Fe(Phen)_2(NCS)_2$, ambient pressure and 0.95 GPa (T = 293 K) for $Fe(Btz)_2(NCS)_2$. (The origin is taken on the iron atom.) [b] Reference 9. [c] Reference 17. [d] This work.

Table VIII. Fe···Fe Distances (Å) between First Neighbors and Angular Orientations (deg) of Fe···Fe Directions with Regard to the Principal Axes of the Lattice[a]

	$Fe(Phen)_2(NCS)_2$		$Fe(Btz)_2(NCS)_2$	
	1000 HPa[b]	1.0 GPa[d]	1000 HPa[c]	0.95 GPa[d]
Fe···Fe(2)	9.35	8.84	8.70	8.36
Fe···Fe(3)	8.31	8.02	8.58	8.28
Fe···Fe(4)	11.08	10.60	11.28	10.98
Fe(2)–Fe–Oy	110.7	110.2	103.5	101.8
Fe(2)–Fe–Oz	20.7	20.2	13.5	11.8
Fe(3)–Fe–Ox	37.7	37.9	39.2	39.2
Fe(3)–Fe–Oy	127.7	127.9	129.3	129.2
Fe(4)–Fe–Ox	53.6	53.4	53.9	54.2
Fe(4)–Fe–Oy	80.8	79.8	72.4	71.3
Fe(4)–Fe–Oz	37.9	38.5	41.4	41.8

[a] Values at ambient pressure and 1.0 GPa (T = 293 K) for $Fe(Phen)_2(NCS)_2$, ambient pressure and 0.95 GPa (T = 293 K) for $Fe(Btz)_2(NCS)_2$. (The origin is taken on the Fe atom.) Fe(2): $-x; -y; -z$; 011. Fe(3): $^1/_2 + x; ^1/_2 + y; ^1/_2 - z; 0\bar{1}0$. Fe(4): $^1/_2 + x; ^1/_2 - y; -z$; 011. [b] Reference 9. [c] Reference 17. [d] This work.

are strongly disordered comparatively to the other carbon atoms, as previously observed at both room and low temperatures.

NCS^- ligands remain almost linear (N(20)–C(21)–S(22) = 179.3°), and are still slightly bent relatively to the Fe–N(20) bond (Fe–N(20)–C(21) = 169.1°, 167.7° at ambient pressure, and 168.0° at 130 K).

2. Crystal Packing. The slight modifications of molecular configuration described above may be accompanied by changes of crystal packing, in terms of molecular rotation and/or translation: these changes will be discussed, along with the intermolecular interactions.

a. Molecular Orientation. The alteration of the coordination core geometry under constraint does not induce significant changes of orientation for $Fe(Phen)_2(NCS)_2$ and $Fe(Btz)_2(NCS)_2$ molecular units relatively to the unit cell axes: Table VII gives the angles between the Fe–N(ligand) bond directions and the unit cell axes a, b, and c, at 1.0 GPa and ambient pressure (T = 293 K). For both compounds, the greatest variations concern N(1)–Fe–Oy angles ($\Delta \simeq 5°$) and N(20)–Fe–Ox angles ($\Delta \simeq 4°$). These variations are very similar to those observed when temperature is lowered from 293 to 130 K at ambient pressure, and owing to their magnitude, they are not expected to modify the intermolecular interactions significantly.

b. Relative Molecular Positions. In order to evaluate the relative displacement of the molecular units, which might occur when applying pressure, we give, in Table VIII, the values at ambient and high pressure of the Fe···Fe distances of the first neighbors, along with the angles between these Fe···Fe directions and the unit cell axes. These values show that the Fe···Fe distances get shorter under the effect of pressure, but the relative positions of the iron atoms do not change.

c. Intermolecular Interactions. It is worth noticing that a 1.0 GPa pressure induces a unit cell volume contraction of ΔV = 269 Å^3 for $Fe(Phen)_2(NCS)_2$ and ΔV = 251 Å^3 for $Fe(Btz)_2(NCS)_2$. These variations are about twice as much as those observed on cooling from 293 to 130 K, i.e. 119 Å^3 for $Fe(Phen)_2(NCS)_2$ and 124 Å^3 for $Fe(Btz)_2(NCS)_2$. Such a unit cell contraction increases the number and the strength of intermolecular contacts: Table IX gives the intermolecular contacts shorter than the van der Waals distances. Let us notice that these contacts include those already observed at room temperature and low temperature (P = 1000 HPa). They are classified into intrasheet and intersheet types, sheets being defined as mentioned above. It is clear that, for $Fe(Phen)_2(NCS)_2$, the number of intrasheet intermolecular contacts is larger than that of intersheet ones; on the contrary, in $Fe(Btz)_2(NCS)_2$, one observes a quasi reverse proportion of the number of intra- and intersheet contacts. Such a behavior was also mentioned in the low-temperature studies. It agrees with the differences observed in the anisotropic lattice thermal expansion of $Fe(Phen)_2(NCS)_2$ and $Fe(Btz)_2(NCS)_2$. In the next section, we will show that this difference in the spatial distribution of intermolecular contacts is correlated with the compressibility data obtained for both compounds in the range 1000 HPa to 1.3 GPa.

Compressibility Data

1. Lattice Parameter Variations. The pressure dependence of lattice parameters are plotted in Figure 3 as fractions of room temperature–ambient pressure values. It can be seen immediately that $Fe(Phen)_2(NCS)_2$ and $Fe(Btz)_2(NCS)_2$ behave differently. In particular, a significant change of derivative is clearly observed on parameter a variation in $Fe(Phen)_2(NCS)_2$, whereas $Fe(Btz)_2(NCS)_2$ lattice parameters show a quasilinear evolution with pressure. Moreover, the lattice parameter c of $Fe(Phen)_2(NCS)_2$ decreases much faster than the one of $Fe(Btz)_2(NCS)_2$. A thorough comparison with thermal dilatation data[17] (as well as with magnetic susceptibility measurements[15] performed under high pressure) allows one to discuss these data more easily.

Table IX. Intermolecular Contacts Shorter than van der Waals Distances for $Fe(Phen)_2(NCS)_2$ at 1000 HPa and 1.0 GPa (T = 293 K) and at 130 K (P = 1000 HPa) and for $Fe(Btz)_2(NCS)_2$ at 1000 HPa and 0.95 GPa (T = 293 K) and at 130 K (P = 1000 HPa)[a]

		$Fe(Phen)_2(NCS)_2$				$Fe(Btz)_2(NCS)_2$		
		1000 HPa		1.0		1000 HPa		0.95
		293 K	130 K	GPa; 293 K		293 K	130 K	GPa; 293 K
		Intrasheet Contacts (Å)						
(2)	C(5)–C(21)		3.50	3.41	C(5)–S(22)			3.55
	C(7)–C(3)	3.53	3.54	3.36				
	C(8)–C(4)		3.55	3.42				
	C(8)–C(5)		3.53	3.40				
	C(9)–C(4)	3.58	3.51	3.39				
	C(9)–C(5)		3.60	3.48				
	C(2)–C(4)			3.58				
	C(6)–C(3)			3.46				
(4)	S(22)–C(12)			3.58	C(10)–S(22)	3.61	3.61	3.48
(5)					S(22)–C(9)			3.52
(6)					C(3)–C(9)			3.56
		Intersheet Contacts (Å)						
(1)	S(22)–C(7)	3.36	3.37	3.16	S(22)–S(6)			3.59
	S(22)–C(8)			3.55				
(3)	C(10)–C(21)			3.59	C(21)–S(7)	3.35	3.27	3.18
					S(7)–S(22)		3.66	3.63
					C(8)–C(21)	3.52	3.45	3.37
					C(2)–S(7)			3.57
					S(7)–S(7)			3.62
					S(7)–N(20)			3.35

[a] Symmetry operations: (1) $^1/_2 + x; ^1/_2 - y; -z; \bar{1}11$. (2) $^1/_2 - x; ^1/_2 + y; z; \bar{1}00$. (3) $-x; -y; -z; \bar{1}00$. (4) $^1/_2 - x; ^1/_2 + y; z$. (5) $x; y; z; 010$. (6) $^1/_2 + x; ^1/_2 + y; ^1/_2 - z; \bar{1}00$.

Let us first consider the case of $Fe(Phen)_2(NCS)_2$. In the thermal dilatation study, a correlation between the spin conversion and the variation of lattice parameters was clearly established; in particular, to the sharp spin transition that occurs at T_c = 176 K, corresponds a sharp variation of the unit cell parameter a. Thus, it seems reasonable to consider that the change of derivative we observe on the same parameter a has to be related to the HS → LS conversion induced under pressure. A polynomial regression analysis of a shows that the change of derivative occurs at a pressure $P \simeq 0.60$ GPa. It is then much tempting to compare our results with those obtained on $Fe(Phen)_2(NCS)_2$ by Usha et al.[15] These authors have performed magnetic susceptibility measurements as a function of both temperature and pressure. The evolution of the HS fraction C_{HS} (%) as a function of pressure, at room temperature, deduced from their results, is plotted on Figure 4 along with that of the unit cell volume found in the present work: it is clearly evidenced that spin conversion and unit cell volume variation are strongly correlated. The critical pressure P_c at 293 K deduced from the C_{HS} curve ($C_{HS}(P_c)$ = 0.5), $P_c \simeq 0.62$ GPa, is very close to our value, viz. 0.60 GPa. This good agreement has been confirmed recently by EXAFS experiments,[14] which yield a transition pressure $P_c \simeq 0.6$–0.7 GPa for $Fe(Phen)_2(NCS)_2$ in form II. The consistency of these recent results questions the data obtained earlier by Fisher,[12] Pebler,[13] Adams,[11] et al. It is not clear whether the discrepancies observed between all these values result from the sample preparation method or the high-pressure experimental conditions used by the authors.

It is interesting to estimate the variation of the unit cell volume only due to the spin crossover. This variation, $(\Delta V_{SC})_P$, has been expressed by Wiehl et al.[20] as the trace of the deformation tensor associated with the LS to HS conversion. In the present case, considering the limited number of data available on $C_{HS}(P)$, one may assume that the total volume variation vs pressure obeys the equation $V(P) = V_o - \Delta V_1 P - (\Delta V_{SC})_P(1 - C_{HS}(P))$ where V_o is the unit cell volume at P = 1000 HPa for 100% HS molecules, ΔV_1 is a linear coefficient which is assumed not to depend on the spin phase considered, $(\Delta V_{SC})_P$ is the unit cell volume variation due to the sole spin crossover, and $C_{HS}(P)$ is the fraction of high-spin molecules, the values of which are taken from ref 15.

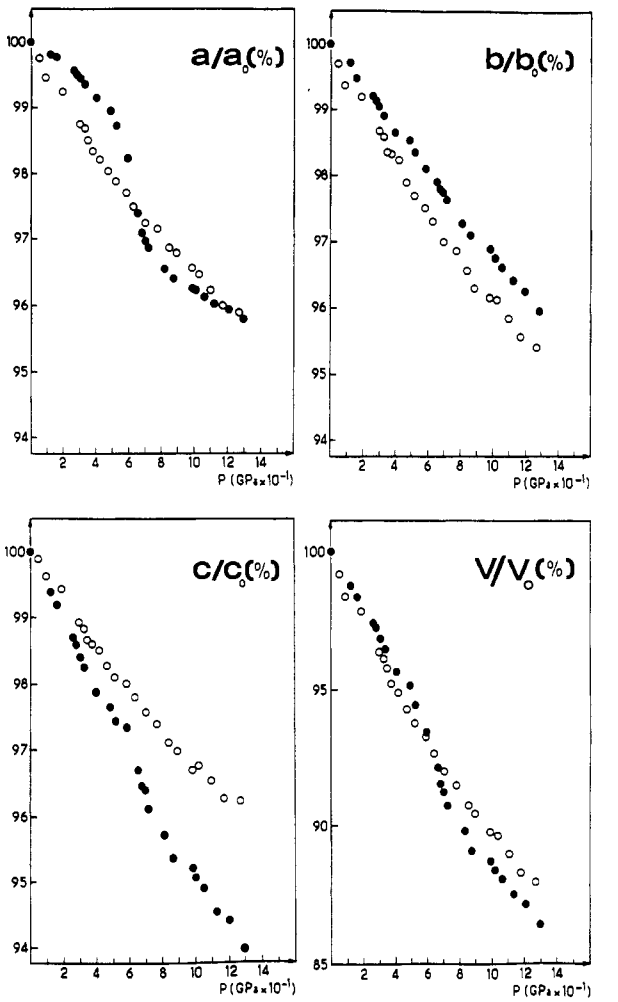

Figure 3. Evolution of the lattice parameters, as fractions of ambient pressure–room-temperature values, at variable pressure: (●) $Fe(Phen)_2(NCS)_2$; (○) $Fe(Btz)_2(NCS)_2$.

Using this equation, the best fit was achieved with the following values: V_o = 2346 Å^3, ΔV_1 = 226 Å^3 GPa^{-1}, and $(\Delta V_{SC})_P$ = 72 Å^3. The V_o value is found to be very close to the one previously measured,[9] viz. 2338 Å, and $(\Delta V_{SC})_P$ is in agreement with the value $(\Delta V_{SC})_T$ = 72 Å^3, deduced previously from variable-temperature experiments.[17]

Concerning $Fe(Btz)_2(NCS)_2$, no drastic anomaly is observed in the 1000 HPa to 1.3 GPa range (see Figure 3): the unit cell parameters decrease almost linearly with pressure. However, one may notice a change of slope in their linear variation, which occurs at a pressure $P \simeq 0.4$ GPa. The lack of physical data at variable pressure does not allow a calculation of $(\Delta V_{SC})_P$, as performed for $Fe(Phen)_2(NCS)_2$. However, an extrapolation, at P = 1000 HPa, of the LS region linear portion of the curve V vs P, yields a volume variation $\Delta V_P = V(1000\ \text{HPa}) - V_{LS}(P = 1000\ \text{HPa})$ = 58 Å^3. This value is certainly underestimated, since it does not take into account the residual fraction of LS molecules which may exist at ambiant pressure and room temperature (8.7% in the present case)[17] as well as the residual fraction of HS molecules at high pressure. Taking into account the 8.7% fraction of LS molecules at ambiant pressure, $(\Delta V_{SC})_P$ is found to be 64 Å^3. However, its real value is expected to be higher. It was estimated at 89 Å^3 in the previous thermal dilatation study.

The analysis of the crystal packing of both complexes in the HS and LS phases shows that $(\Delta V_{SC})_P$ and $(\Delta V_{SC})_T$ are directly related to the changes of octahedron geometry associated with

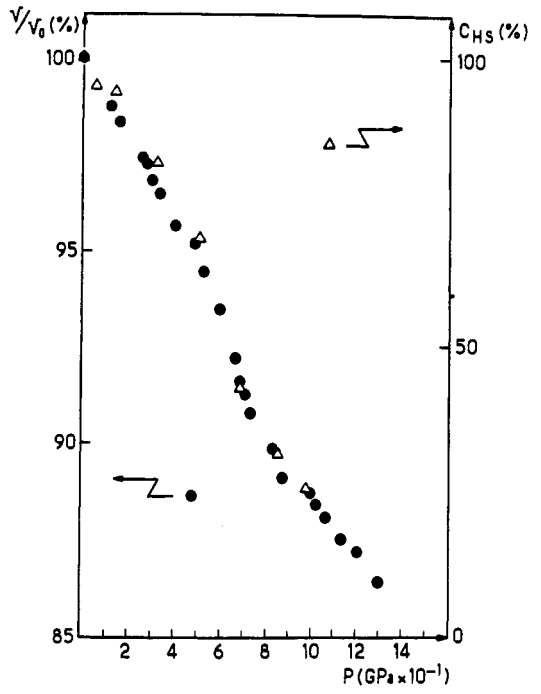

Figure 4. Pressure dependence of the unit-cell volume (as fraction of ambient pressure–room-temperature value) and of the high-spin fraction C_{HS} (%) (deduced from Usha et al.[15] data) for $Fe(Phen)_2(NCS)_2$.

Table X. Linear and Volumic Compressibility Coefficients (10^{-1} GPa^{-1}) of $Fe(Phen)_2(NCS)_2$ and $Fe(Btz)_2(NCS)_2$ at Two Different Pressures: 1000 HPa and 1.0 GPa

	$Fe(Phen)_2(NSC)_2$	$Fe(Btz)_2(NSC)_2$
	P = 1000 HPa	
k_a	0.21	0.41
k_b	0.33	0.43
k_c	0.53	0.37
k_v	1.07	1.21
	P = 1.0 GPa	
k_a	0.16	0.28
k_b	0.28	0.33
k_c	0.38	0.28
k_v	0.82	0.89

the spin crossover, i.e. to Fe–N(ligand) bond length shortening, and that they do not include a strong contribution of molecular packing rearrangement.

One may then conclude that, at least in the case of $Fe(Phen)_2(NCS)_2$, ΔV_{sc} does not depend on the applied constraint.

2. Linear and Volumic Compressibility Coefficients. From the lattice parameter variations, one may deduce the values of linear and volumic compressibility coefficients. These are given in Table X for high- and low-pressure regions, where HS to LS conversion can be considered as negligible (except in the case of $Fe(Btz)_2(NCS)_2$, for the low-pressure region).

A significant anisotropy is observed in the linear coefficients of $Fe(Phen)_2(NCS)_2$, whereas $Fe(Btz)_2(NCS)_2$ exhibits an almost isotropic compressibility. The anisotropy of $Fe(Phen)_2(NCS)_2$ is slightly reduced at high pressure; however, a remains the stiffest direction while c is the more compressible one. Qualitatively, there is a certain correlation between such a lattice anisotropy and the spatial distribution of intermolecular contacts (see Table VIII). In the case of $Fe(Phen)_2(NCS)_2$, the lowest values of linear compressibility, which are associated with stiffest lattice directions, concern axes a and b: these correspond to intrasheet directions in which one observes many intermolecular contacts; k_c, on the other hand, is larger than k_a and k_b, and corresponds to the intersheet direction for which many fewer contacts are observed. In the case of $Fe(Btz)_2(NCS)_2$, the proportion of inter- and intrasheet contacts is almost reversed, and one observes a quasi-isotropic lattice with respect to pressure effects.

Finally, both complexes exhibit very close values of volumic compressibility, at low and high pressure, $Fe(Phen)_2(NCS)_2$ being only a little stiffer than $Fe(Btz)_2(NCS)_2$: $k_v(Btz)/k_v(Phen) \simeq 1.10$. Considering that the k_v value for $Fe(Btz)_2(NCS)_2$, at low pressure, does not entirely correspond to the isothermal compressibility of the pure HS phase, one may conclude that the bulk modulus K ($K = 1/k_v$) of $Fe(Btz)_2(NCS)_2$ is not significantly lower than that of $Fe(Phen)_2(NCS)_2$.

Spiering et al.[19] have proposed a model based on elasticity theory, in which the sharpness of the spin transition as a function of temperature is related to the stiffness of the crystal lattice. Adler et al.[21] have used this model for interpreting the experimental data obtained on two compounds: $[Fe(2\text{-pic})_3]Cl_2$·MeOH (gradual transition compound) and $[Fe(2\text{-pic})_3]Cl_2$·EtOH (less gradual transition compound). A value of ≈ 1.3 for the bulk moduli ratio $K(EtOH)/K(MeOH)$ is then required so as to fit the model. The experimental values of the bulk moduli deduced from the Lamb–Mössbauer factors at room temperature lead to a ratio of $\simeq 1.12$. The authors suggest that a better agreement with the model should be obtained by taking into account the anisotropy of the lattice, which they observed on the linear thermal expansion coefficients. In our case the bulk moduli ratio is $K(Phen)/K(Btz) = k_v(Btz)/k_v(Phen) \simeq 1.0$ at both low and high pressure. Our compressibility data show that the crystal lattice of $Fe(Phen)_2(NCS)_2$ exhibits a marked anisotropy compared to that of $Fe(Btz)_2(NCS)_2$. This difference was also observed from the linear thermal expansion coefficients of the two compounds and is related to the difference observed in the spatial distributions of their intermolecular contacts.

Conclusion

We have carried out a single crystal X-ray diffraction investigation, at variable pressure, on two isostructural iron(II) spin-transition complexes, $Fe(Phen)_2(NCS)_2$ (form II) and $Fe(Btz)_2(NCS)_2$, presenting different HS $\leftrightarrow$ LS transition characteristics:

$Fe(Phen)_2(NCS)_2$ was known to exhibit a spin crossover either at ambient pressure and T_c = 176 K (discontinuous transition), or at room temperature and high pressure, the transition pressure P_c being still debated.

$Fe(Btz)_2(NCS)_2$ was reported to show a gradual spin conversion as a function of temperature, centered at $T_c \simeq 225$ K, while its behavior as a function of pressure had not yet been investigated.

This study is the continuation of a similar investigation performed as a function of temperature.[9,16,17] It makes more complete the structural data obtained on these two complexes and reveals the common points and the differences on their structural properties.

Both complexes remain in the space group *Pbcn* over the whole pressure range of 1000 HPa to 1.3 GPa, just as no change in the space group was observed for the temperature range of 130–300 K.

The full structure determinations performed at $P \simeq 1.0$ GPa show that they exhibit very similar intramolecular modifications under pressure, which essentially concern [Fe–N_6] octahedron geometry. Moreover, the shortening of the Fe–N(ligand) bond lengths, and the variation of the N(ligand)–Fe–N(ligand) bond angles are very close to the ones observed when passing from room temperature to low temperature. This leads us conclude that the change of molecular configuration when going from the HS to the LS state does not depend significantly on the applied constraint, temperature or pressure.

The compressibility data obtained in the pressure range 1000 HPa to 1.3 GPa allows us, by comparison with the thermal expansion data determined previously, to assert the following points:

The transition pressure P_c found for $Fe(Phen)_2(NCS)_2$ is detected by the change of derivative in the curve representing the

variation of parameter *a* as a function of pressure, which occurs at ≃0.6 GPa. This result is in good agreement with the magnetic susceptibility data obtained by Usha et al.,[15] as well as with the near-edge X-ray absorption experiments performed by Roux et al.[14]

The HS to LS conversion appears to be more gradual in the case of $Fe(Btz)_2(NCS)_2$ and seems to mainly take place between 1000 HPa and 0.6–0.7 GPa. However, this statement has to be confirmed by carrying out experiments involving physical properties.

For $Fe(Phen)_2(NCS)_2$, the volume change $(\Delta V_{SC})_P$ upon the spin transition is found to be the same as $(\Delta V_{SC})_T$.

Both compounds have very similar volumic compressibility coefficients, either in the low- or in the high-pressure region, $Fe(Phen)_2(NCS)_2$ being a little stiffer than $Fe(Btz)_2(NCS)_2$.

The only noticeable difference in the evolution of the structural properties of these two compounds as a function of pressure is that $Fe(Phen)_2(NCS)_2$ exhibits a strong lattice anisotropy compared to $Fe(Btz)_2(NCS)_2$. This lattice anisotropy is well correlated with the number and the spatial distribution of the shortest intermolecular distances. These results do not contradict the model proposed by Spiering et al.[19] and lend some support to the conclusions drawn by Adler et al.,[21] where these authors suggest that lattice anisotropy has to be taken into account in the intermolecular interaction energy.

Supplementary Material Available: Table SI, giving details on high-pressure data collection characteristics, Table SIIa,b, giving calculated fractional positions and isotropic thermal parameters for hydrogen atoms and anisotropic thermal parameters for non-hydrogen atoms for $Fe(Phen)_2(NCS)_2$ and $Fe(Btz)_2(NCS)_2$, respectively, and Table SIIIa,b, giving lattice parameters of $Fe(Phen)_2(NCS)_2$ and $Fe(Btz)_2(NCS)_2$ respectively, measured at 293 K as a function of pressure, in the range 1000 HPa to 1.3 GPa (7 pages). Ordering information is given on any current masthead page.